Part 5. Non-Spherical Mass Loss, Binarity, Post-AGB Evolution

https://doi.org/10.1017/S0074180900203343 Published online by Cambridge University Press

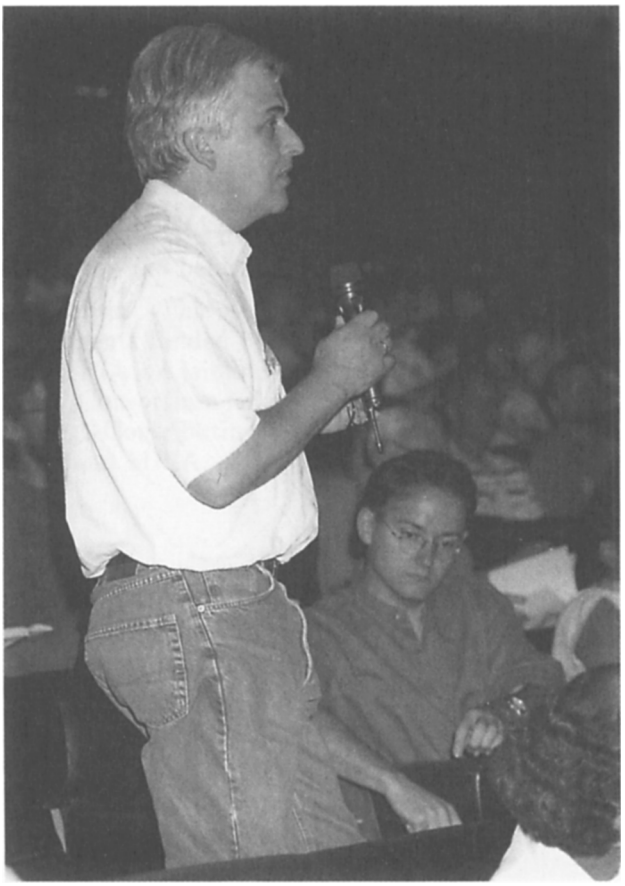

Gerd Weigelt commenting on high-angular resolution

https://doi.org/10.1017/S0074180900203343 Published online by Cambridge University Press

Asymptotic Giant Branch Stars
T. Le Bertre, A. Lèbre and C. Waelkens, eds.
I.A.U. Symposium 191, 1999

AGB and post-AGB stars at high angular resolution

Bruno Lopez

Observatoire de la Côte d'Azur, Département Fresnel UMR 6528, BP 4229, F-06034 Nice Cedex 4, France

Abstract.

High angular resolution observations have provided some valuable information on the circumstellar environment of AGB and post-AGB stars.

We review the recent results obtained in this field and focus on observations showing evidence of non-sphericity at different spatial scales (envelope, jets, binarity, maser clumps, stellar "photosphere", hot spots, etc.). Such studies provide many informations/constraints not yet fully understood and seldom included in models.

Although the available observations are very nice and interesting, they sometimes show limited performances with regards to what is needed to analyse the onset of the winds. We try to show, here, what must be gained to improve our present knowledge.

1. Introduction

The mass loss of Asymptotic Giant Branch (AGB) stars plays an important role during this late stage of their evolution. One of the major questions raised in this field of research concerns the mechanisms producing the mass loss. There are, in my opinion, two obstacles which prevent to easily observe what causes the mass loss phenomenon (see Fig. 1):

- the mass loss is a combination of several mechanisms → their different contributions are difficult to disentangle;
- the signatures of the wind(s) begin at the stellar surface → ideally the photospheric layers should be angularly resolved.

To explain the mass loss phenomenon, a general picture including two mechanisms is presently admitted: the gas is, in a first step, levitated at a distance large enough to allow the formation of dust particles, then, the radiation pressure drives away the dust which drags the gas in its expanding outward motion. Despite the interest of this picture, the physical conditions that favour the mass loss activity and create the commonly observed asymmetries, are still not well understood.

In this review, we are pointing out a number of issues to address with the high angular resolution methods:

- When do asymmetries occur during the stellar evolution ?
- How are interpreted the non-spherical envelopes ?
- What may be the causes of departures from spherical symmetry ?
- What is observed during the superwind phase ?

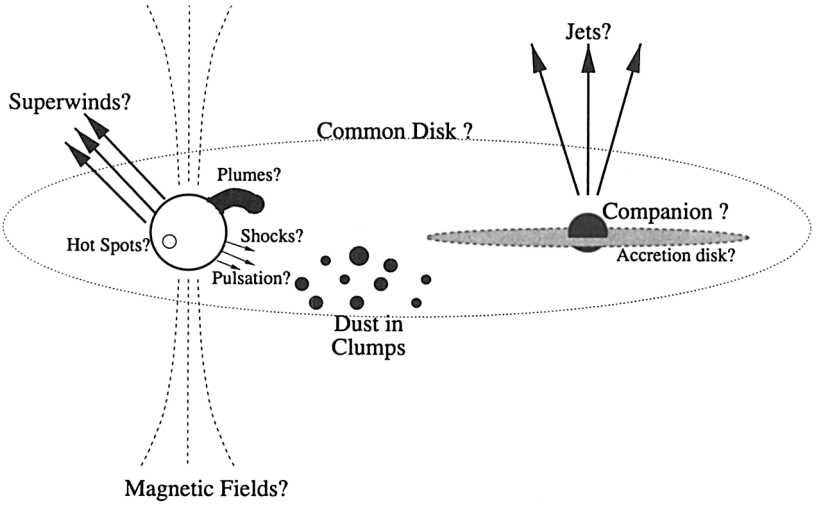

Figure 1. Sketch of the expected circumstellar environment of an AGB star. One stellar radius is between about 10 and 20 mas for the most nearby stars (located at a distance of a few hundred parsecs). Dust grain nucleation occurs at a distance of a few stellar radii from the star.

- What kind of clumpiness is observed ?
- What is observed at the stellar surface level ?

We will try, whenever possible, to link the observations and the theoretical models. However, this presentation will not be exhaustive. Observational results based on polarimetric measurements will not be covered here (see Magalhães & Nordsieck 1998), nor the observational results on massive cool supergiant stars, although some of the physical conditions in their circumstellar environment are probably similar to those of AGB stars.

2. When do asymmetries occur during the stellar evolution ?

Several observational studies show that an important fraction of AGB and/or post-AGB sources are asymmetric. For example, the ^{12}CO atlas of circumstellar envelopes of AGB and post-AGB stars (Neri et al. 1998) contains 46 objects. Interferometric visibility curves obtained with the IRAM interferometer are combined with short spacing observations from the IRAM 30 m telescope. Within the sensitivity of these observations, there is evidence for a significant asymmetry in about 30 percents of the detected envelopes. One can also refer to other recent papers such as the study of Sánchez Contreras et al. (1998)

https://doi.org/10.1017/S0074180900203343 Published online by Cambridge University Press

in which the extended cold dust emission at 1.3 mm has been observed for a sample of 16 evolved stars, the mid-infrared observations of Busso et al. (1996), the mid-infrared survey of Meixner et al. (1998a, 1998b) showing two typical morphologies (toroïdal versus elliptical) for 66 PPNe.

Aside from these different observations which reveal that asymmetries occur for a non-negligible fraction of the sources, a deeper analysis is presently required to understand when (and why) are asymmetries occurring during the stellar evolution ? More precisely, does the asymmetric matter distribution rather occur at the tip of the AGB in the transition phase to a planetary nebula or does it occur during the AGB at the first mass loss stages ?

Some important clues for an envelope morphology possibly changing at the tip of the AGB are encountered in the envelope of CW Leo (IRC+10216). The envelope is detected out to a distance of 50 arcsec in the 1.3 mm continuum emission (Groenewegen et al. 1997) and about twice this distance in the visible wavelengths (de Laverny et al. 1998), corresponding to a dynamic time scale of about 6 000 years. The large outer shell of CW Leo is spherical in contrast with the inner core of asymmetric shape (Le Bertre et al. 1989; Hannif & Busher 1998; Weigelt et al. 1998a; Weigelt et al. 1999; Tuthill et al. 1998b; Tuthill et al. 1999). This may suggest that the geometry of the wind has changed during its history and may indicate that the asymmetries seen in most planetary nebulae and preplanetary nebulae are already established before the progenitor stars have left the AGB.

Asymmetries are also detected in other carbon stars such as CIT6 (Trammel & Goodrich 1998; Tuthill et al. 1998c) and IRAS 06088+1909 (Richichi et al. 1998). The source OH 231.8+4.2 which is the host of a Mira variable star has also a very well marked bipolar shape (Kastner et al. 1998; Kastner et al. 1999). In K band, its northern and southern lobes are resolved into jet like-fingers. As for CW Leo and CIT6, this source is probably at the tip of the AGB, in a brief transition stage of evolution: just before the central AGB star reaches a warmer photospheric effective temperature that characterizes the post-AGB stars.

One may wonder if similar asymmetrical features are encountered at the first mass loss stages, if they are common and what are the epoch of their onset ?

To our knowledge, asymmetries are not yet clearly detected before the star reaches the tip of the AGB (high mass loss rate). As a personnal experience, we performed a study using the University of California at Berkeley Interferometer on the Mira *o* Ceti. We had to consider several non-spherical geometries of the envelope in our radiative transfer model in order to fit the 10 μm visibility curves (Lopez et al. 1997b). But these geometries remain hypothetical because the observational contraints are not strong enough to determine a "unique" solution. In other words, during the first stages of the mass loss, when the mass loss rate is low or moderate, the dust shell is very thin and cannot be as easily observed as it is for the envelopes of PPNs or objects like the carbon-rich star CW Leo.

Answering to when does asymmetries occur, therefore requires to observe the dust shell geometry of Mira stars during the first stages of their mass loss episode. This goal will be actually achieved by using the next generation infrared or optical interferometers. These interferometers will allow a good Fourier plane coverage with possibly an imaging capability.

3. How are interpreted the non-spherical envelopes ?

It appears that the geometry of the envelopes cannot be easily defined, even when the large spatial structures of the envelopes are angularly well resolved. It is the case, for example, of the nearest post-AGB nebulae such as the Egg Nebula and the Red Rectangle. Their morphology has been interpreted in various ways by several authors, proposing:

- a bipolar dust shell with a thick equatorial disc of sharp edges (Dyck et al. 1987);
- a dust shell with an azimuthal density distribution varying in a smooth way above and below the equatorial plane (Collison & Fix 1991; Lopez et al. 1997a);
- an hybrid dust envelope composed by an initially spherically symmetric AGB wind combined with an axially symmetric superwind phase of enhanced mass loss in the equatorial plane, or in the perpendicular direction ? (Meixner et al. 1997);
- a spherical dust envelope with bipolar wind blown holes (Whitney & Hartmann 1993; Sahai et al. 1998a).

Among these various interpretations, a commonly accepted characteristic is the presence of a torus or a disk-like distribution of matter, consistent with the shape of many nebulae. The carbon-rich Egg Nebula, for example, has been observed using aperture synthesis method in several molecular lines (Nguyen-Q-Rieu & Bieging 1990). These observations are consistent with a toroidal geometry for the expanding envelope, that was originally inferred from optical scattering model (Yusef-Zadeh et al. 1984) and confirmed by more recent investigations (Skinner et al. 1997; Lopez & Perrin 1998a). HST high angular resolution near-infrared and visible images of the bipolar protoplanetary nebula CRL 2688 are reported in Sahai et al. (1998a). The emergence of the bipolarity of objects like the Egg Nebula is believed to be intimately connected to the formation and preexistence of a dusty cocoon concentrated toward the equatorial plane and with the interaction of a high velocity collimated outflow. The pre-cited data seem to provide evidence for both phenomena.

Some axisymmetric radiative transfer modelling were used to understand the geometry of the Red Rectangle nebula (Weigelt et al. 1998b; Weigelt et al. 1999; Lopez et al. 1997a). These models are based on high angular resolution observations, such as those obtained in near-infrared by Cruzalèbes et al. (1996) and in visible light by Osterbart et al. (1997). The Red Rectangle appears as an extended (up to 40 arcsec) reflecting nebula with a pronounced bipolar structure. The extension of the dark lane in the East-West direction allows to derive a lower limit for the outer radius of the dust disk of at least 65 AU and since there is no reddening of the fainter northern lobe, an upper limit of 200 AU can roughly be estimated (Weigelt et al. 1998b).

Furthermore, Waters et al. (1998) report ISO observations of the Red Rectangle revealing the presence of oxygen-rich materials similar to those found in dusty disks surrounding young stars. Grain processing and perhaps even planet formation may therefore also be occurring in the circumbinary disk of this evolved star. An evolutionary scenario is proposed in which the disk is the result of extensive mass transfer and/or mass loss while the star was still

oxygen-rich. In the circumstellar environment of the Red Rectangle, Jura et al. (1997) have detected some big grains and have shown that the most plausible interpretation of the CO velocity profile is that it signals the presence of a long lived orbiting disk.

It can be concluded that the large scale structures observed in all the bipolar nebulae (the lobes) are rather well modelled and related to a concentration of material in an equatorial plane. However the present observations and the plausible models do not yet give precisely the exact inner geometry: disk, torus or cocoon ? Understanding the inner geometry remains a goal of importance since it should provide some relevant signatures on the origin(s) of asymmetries.

4. What may be the causes of departure from spherical symmetry ?

Asymmetries in the envelopes could have different origins which can be connected to:

- the rotation of the star,
- the magnetic fields,
- the presence of a companion.

The CO lines of V Hya suggest that it is rotating with a *vsini* between 10-20 km/s (Kahane et al. 1988). In addition, the radio map of its circumstellar envelope is clearly anisotropic and presents a bipolar component. According to Kahane et al. (1988), the anisotropy in the outflow from V Hya seems to result from the rotation of the star.

Magnetic field probably combined with stellar rotation may also produce asymmetries (Soker 1998). The SRa star W Hya shows strong circular polarization (Szymczak et al. 1998) in its OH emission spectrum. Masers with close spatial coincidence and opposite circular polarization lead to an estimate of the magnetic field of 0.6 mG at 80-130 AU from the star. The strength of the magnetic field at the stellar surface could reach about 10 G. Furthermore, in W Hya the blue-red shifted velocity gradient appears to be caused by a density enhancement towards the equatorial plane.

Aside, the most often invoked cause of asymmetry is the binarity. Direct evidence is found supporting a binary star formation mechanism for the Frosty Leo nebula (Roddier et al. 1995). According to Morris (1987), Morris (1981), Iben et al. (1993) and recently Mastrodemos (1998), a second star would attract the material ejected by the red giant and form an accretion disk. This has two consequences. Firstly, dust tends to accumulate in the orbital plane, obscuring both stars when the orbit is seen edge-on. Secondly, a fast polar wind is created on the second star and could blow out dust on each side of the disk. This second wind may be the cause of formation of the search-light beam observed in the Red Rectangle and the Egg Nebula (Sahai et al. 1998a). An indirect detection by spectrometric Doppler shift of a binary at the heart of the Red Rectangle has also been reported (Van Winckel et al. 1995; Walkens et al. 1996).

Jura & Turner (1998) report high angular resolution observations at millimeter and submillimeter wavelengths of the dust disk associated with the Red Rectangle. A dust clump with an estimated mass near that of Jupiter in the outer region of the disk is observed. The clump located at 4.3 arcsec from the primary (1600 AU) is larger than the Solar System and its nature is at present

unclear. Sahai et al. (1998) report high resolution near-infrared images and polarimetric images of the inner region of the bipolar protoplanetary nebula CRL 2688. The polarization map yields the probable detection of a companion. Its measured projected separation is 750 AU. This may lend additional weight to binary based models.

Furthermore, the indirect evidence of an accretion disk around a companion has been realized for Mira (*o* Ceti). Warner (1972) has shown that the companion luminosity is flickering and suggests the presence of an accreting material. It is shown that considering the circumstellar density of the gas, the kinetic energy transformed in the accretion process could easily produce the companion luminosity. This binary has also been observed by Karovska et al. (1997) using the HST (see also Karovska 1999). The dust shell observed in the J band by means of adaptive optics possibly shows that the companion has some effects on the shape of the dust envelope, but this has to be confirmed (Lopez et al. 1998b).

Presently, among the proposed mechanisms (stellar rotation, magnetic field, binarity), the main cause of envelopes departures from spherical symmetry is not clearly defined. The binarity however seems to be the easiest hypothesis to check at the present time from an observational point of view.

5. What is observed during the superwind phase ?

Observations of the superwind phase show an enhanced mass loss rate associated with a high velocity wind. Atomic and molecular emission lines are produced by the superwind when it encounters the low velocity AGB wind. The geometry of the envelopes observed during this phase is asymmetrical. It is not known if the geometry of the superwind is intrinsically related to the properties of the star itself or if it mostly results from an interaction with the remnants of the AGB envelopes.

The well resolved morphology of IRAS 07134+1005 shows an elliptical outer shell surrounding two aligned peaks. They are interpreted as limb brightened peaks of an optically thin elliptical shell with an equatorial density enhancement (Meixner et al. 1997). Using a code describing the axial symmetry of the dust shell, the dust emission images and the spectral energy distribution of four other PPNe such as IRAS 07134+1005 are modelled. The dynamical age estimates indicate that these stars have left the AGB 300-1 400 years ago, just after the superwind phase. In order to match with the models the 60 and 100 μm photometry, the AGB mass loss rate has to be about 20 times smaller than the superwind mass loss rate. Taking into account the distance uncertainties, the superwind mass loss rate ranges between 10^{-4} and 10^{-6} $M_{\odot}yr^{-1}$.

M1-92 is probably the PPN for which the structure and properties of the wind interaction, the dominant formation process of PN, are being studied in most details (Alcolea & Bujarrabal 1999). HST imaging of continuum and atomic lines (H_{α}, [OI], [SII] and [OIII]) are presented in Bujarrabal et al. (1998), see also Trammel & Goodrich (1996). Ground based imaging of the 2 μm continuum and H_2 ro-vibrational (S(1) v = 1–0 and v = 2–1) lines has also been performed. The optical line emissions come mainly from two chains of shocked knots placed along the symmetry axis of the nebula and inside those cavities

https://doi.org/10.1017/S0074180900203343 Published online by Cambridge University Press

for which relatively high excitation is deduced allowing the estimate of a shock velocity of about 200 km/s. The hollow shape of the CO lobes strongly suggests the effect of a wind interaction between the fast bipolar outflow presently ejected by the star and the slow dense envelope ejected during the past AGB-phase. The line emission images show several knots of emitting material that are not present in the continuum map. Such clumps are mostly located in the axis of the nebula and placed symmetrically at about 2.2 and 3.3 arcsec from the star. The clumpy image of this bipolar flow is similar to the sinuous chain of knots often mapped in jets associated to young stellar objects (Reipurth 1989). The big contrast between the emission from the bipolar jet and the emission from the bow leading shock may indicate that the jet density is smaller than that of the AGB shell by a factor larger than 10.

6. What kind of clumpiness is observed ?

Movies were presented during the Symposium by Diamond & Kemball (1999) and Richards et al. (1999) for two types of maser spots (SiO and H_2O, resp.). These very beautiful results allow the study of the velocity fields near the stars, and the analysis of the acceleration process on dust by radiation pressure.

Observations of TX Cam and U Her at 43 GHz (SiO masers) using the VLBA reveal well defined rings of spot emissions at 2-4 stellar radii (Diamond & Kemball 1999; Diamond et al. 1994). The masers appear to lie in the so called extended atmosphere, the region between the photosphere and the dust formation point. IR interferometry on such AGB stars (Danchi et al. 1994) indeed reveals that dust condenses at a few stellar radii (3-5) from the center of the star, while SiO masers are not located beyond 4 stellar radii. Presumably, this is the radius at which, Si atoms begin to condense into dust.

Filaments of water maser spots (about 1 km/s and 10-20 mas long) are observed in the dust shell of RT Vir (once the dust has already condensed). The distribution of the 22 GHz water maser spots (Bains 1995) shows a systematic red-shift of the masers to the East and a blue shift to the West. This suggests that the source may have an intrinsic bipolarity.

Because of instrumental limitations, while hundreds of maser spots and their motions are observed, only a few clumps of dust are clearly detected close to a star (i.e. at a distance were dust condensation has occurred during the recent mass loss history). About 4 clumps of dust are observed around the carbon star CW Leo (Haniff & Busher 1998; Tuthill et al. 1998b; Tuthill et al. 1999; Weigelt et al. 1998a; Weigelt et al. 1999). Considerable changes have occurred in the morphology of CW Leo in the past 8 years: whereas in 1989 both the K and L band emissions were apparently dominated by a single core, in 1997 there were four compact components.

These results are exciting and the still improving observational methods should allow in the future to study the dust formation region and its clumpiness. The clumps of CW Leo appear to move outward and offer the perspective to better understand the contribution of the radiation pressure to the mass loss and the physical conditions under which dust forms near the star.

7. What is observed at the stellar surface level ?

Observations of the stellar surface and its changes with time are crucial to understand the origin of mass loss. To the best of my knowledge there are only a few relevant direct observations of the stellar surfaces. This is because ideally they require the use of long baseline interferometry methods which are not yet able to perform image reconstructions at optical or infrared wavelengths. The presence of shock waves, hot spots, stellar distorsions or plumes is expected and need to be studied in deep details (see Fig. 1).

The photospheric surfaces of five long period variables (o Ceti, R Leo, W Hya, χ Cyg and R Cas) have been imaged in the optical/near-IR at the 4.2 m William Herschel Telescope (Tuthill et al. 1998a). All these sources exhibit departures from circular symmetry. Good fits of the data could be attained with bright spots models, but the detailed parameters - brightness and locations of the spots - are very poorly constrained. The use of a bright-spots model does not rule out the interpretation of a possible elliptical photosphere. Moreover, stellar morphologies change markedly from one epoch to another. Such changes are graphically evident in the Fourier data obtained at two epochs on o Ceti. Secular changes in the shape of o Ceti have been also interpreted by elliptical models (Karovska et al. 1991; Quierrenbach et al. 1992) giving a variable position angle and axial ratio. The observations of Tuthill et al. (1998a) have revealed that changes in the appearance of o Ceti are the result of the evolution of bright features rather than gross distorsions of the overall stellar atmosphere. The time scale for this evolution would seem to lie somewhere between 3 and 14 months.

Observations of the photospheric surface of Miras made with large aperture telescope are also presented by Hofmann et al. (1998) and by Karovska et al (1997). The image of o Ceti observed in the UV light by the HST is spectacular. It shows a plume like feature that points toward the companion position. To my knowledge, the direct imaging of such a plume feature is unique for a star other than the Sun. The physical reasons for the occurrence of this feature is not clear.

8. Conclusion

It is of crucial importance to study the geometry of the envelopes during the first episodes of the mass loss process, when the mass loss rate is low or moderate. This leads to a better understanding of when and why the asymmetries occur.

To my opinion, very nice observational results have been obtained up to now by means of high angular resolution methods. However, the best remains to be done. The interferometers such as the ISI, the VLTI and the Keck are expected to bring strong observational constraints on the stellar photospheres and on the circumstellar regions near the photosphere, where the mass loss starts.

I am impressed by the very nice movies obtained by radio interferometric method on maser clump motions. Because the objects we study are alive, it seems necessary not only to image the circumstellar environments with as many details as possible, but also to monitor all the physical processes encountered and to determine their typical lifetime scales.

Acknowledgments. Thanks to G. Niccolini for help in the reading of some papers during the preparation of this review. N. Epchtein and P. de Laverny were kind to read and comment this paper before publication.

References

Alcolea J., Bujarrabal V., 1999, this volume

Bains I., 1995, MSc thesis, University of Manchester

Danchi W.C., Bester M., Degiacomi C.G., Greenhill L.J., Townes C.H., 1991, ApJ 367, L27

Bujarrabal V., Alcolea J., Sahai R., Zamorano J., Zijlstra A.A., 1998, A&A 331, 361

Busso M., Origlia L., Marengo M., et al., 1996, A&A 311, 253

Collison A., Fix J.D., 1991, ApJ 368, 545

Cruzalèbes P., Lopez B., Bester M., Gendron E., Sams B., 1996, A&AS 116, 597

de Laverny P., Mauron N., Lopez B., 1998, poster contribution, this conference

Diamond P.J., Kemball A.J., Junor W., et al., 1994, ApJ 430, L61

Diamond P.J., Kemball A.J., 1999, this volume

Dyck H.M., Zuckerman B., Howell R.R., Beckwith S., 1987, PASP 99, 99

Groenewegen M.A.T., van der Veen W.E.C.J., Lefloch B., Omont A., 1997, A&A 322, L21

Haniff C.A., Buscher D.F., 1988, A&A 334, L5

Hofmann K.-H., Weigelt G., Balega Y.Y., Scholz M., 1998, AGM 14, 52

Iben I., Jr., Livio M., 1993, PASP 105 1373

Jura M., Turner J., Balm S.P., 1997, ApJ 474, 741

Jura M., Turner J., 1998, Nature 395, 144

Kahane C., Maizels C., Jura M., 1988, ApJ 328, L25

Karovska M., 1999, this volume

Karovska M., Hack W., Raymond J., Guinan E., 1997, ApJ 482, L175

Karovska M., Nisenson P., Papaliolios C., Boyle R.P., 1991, ApJ 374, L51

Kastner J.H., Weintraub D.A., Merrill K.M., Gatley I., 1998, AJ 116, 1412

Kastner J.H., Henn L., Weintraub D.A., Gatley I., 1999, this volume

Le Bertre T., Magain P., Remy M., 1989, The ESO Messenger 55, 25

Lopez B., Tessier E., Cruzalèbes P., Lefèvre J., Le Bertre T., 1997a, A&A 322, 868

Lopez B., Danchi W.C., Bester M., et al., 1997b, ApJ 488, 807

Lopez B., Perrin J.M., 1998a, A&A, in preparation

Lopez B., Cruzalèbes P., Aristidi E., et al., 1998b, A&A, in preparation

Magalhães A.M., Nordsieck K.H., 1998, in "The carbon star phenomenom", IAU Symposium 177, ed. R. Wing, in press

Mastrodemos N., 1998, Ph.D. thesis, University of California

Meixner M., Skinner C.J., Graham J.R., et al., 1997, ApJ 482, 897

Meixner M., Ueta T., Dayal A., et al., 1998a, submitted to ApJ
Meixner M., Ueta T., Dayal A., et al., 1998b, poster contribution, this conference
Morris M., 1987, PASP 99, 1115
Morris M., 1981, ApJ 249, 572
Neri R., Kahane C., Lucas R., Bujarrabal V., Loup C., 1998, A&AS 130, 1
Nguyen-Q-Rieu, Bieging J.H., 1990, ApJ 359, 131
Osterbart R., Langer N., Weigelt G., 1997, A&A 325, 609
Quierrenbach A., et al., 1992, A&A 259, L19
Reipurth B., 1989, ESO Workshop on "Low mass stars formation and pre-main sequence objects", ed. B. Reipurth, p. 247
Richards A.M.S., Cohen R.J., Bains I., Yates J.A., 1999, this volume
Richichi A., Stecklum B., Herbst T.M., Lagage P.-O., Thamm E., 1998, A&A 334, 585
Roddier F., Roddier C., Graves J.E., Northcott M.J., 1995, ApJ 443, 249
Sahai R., Hines D.C., Kastner J.H., et al., 1998, ApJ 492, L163
Sánchez Contreras C., Alcolea J., Bujarrabal V., Neri R., 1998, A&A 337, 233
Skinner C.J., Meixner M., Barlow M.J., et al., 1997, A&A 328, 290
Soker N., 1998, MNRAS 299, 1242
Szymczak M., Cohen R.J., Richards A.M.S., 1998, MNRAS 297, 1151
Trammel S.R., Goodrich R., 1996, ApJ 468, L107
Trammel S.R., Goodrich R., 1998, private comunication
Tuthill P.G., Haniff C.A., Baldwin J., 1998a, submitted to MNRAS
Tuthill P.G., et al., 1998b, in preparation
Tuthill P.G., et al., 1998c, in preparation
Tuthill P.G., Monnier J.D., Danchi W.C., 1999, this volume
Van Winckel H., Waelkens C., Waters L.B.F.M., 1995, A&A 293, L25
Waelkens C., Van Winckel H., Waters L.B.F.M., Bakker E.J., 1996, A&A 314, L17
Warner B., 1972, MNRAS 159, 95
Waters L.B.F.M., Waelkens C., Van Winckel H., et al., 1998, Nature 391, 868
Weigelt G., Balega Y.Y., Bloecker T., et al., 1998a, A&A 333, L51
Weigelt G., Balega Y.Y., Men'shchikov A.B., Osterbart R., 1998b, submitted to New Astronomy
Weigelt G., Blöcker T., Hofmann K.-H., et al., 1999, this volume
Whitney B.A., Hartmann L., 1993, ApJ 402, 605
Yusef-Zadeh F., Morris M., White R.L., 1984, ApJ 278, 186